

Studies on the Reaction Mechanism of *Rhodotorula gracilis* D-Amino-acid Oxidase

ROLE OF THE HIGHLY CONSERVED Tyr-223 ON SUBSTRATE BINDING AND CATALYSIS*

(Received for publication, May 21, 1999, and in revised form, September 7, 1999)

Christopher M. Harris‡, Gianluca Molla, Mirella S. Pilone, and Loredano Pollegioni§

From the Department of Structural and Functional Biology, University of Insubria, via J. H. Dunant 3, 21100 Varese, Italy

We have studied D-amino-acid oxidase from *Rhodotorula gracilis* by site-directed mutagenesis for the purpose of determining the presence or absence of residues having a possible role in acid/base catalysis. Tyr-223, one of the very few conserved residues among D-amino-acid oxidases, has been mutated to phenylalanine and to serine. Both mutants are active catalysts in turnover with D-alanine, and they are reduced by D-alanine slightly faster than wild-type enzyme. The Tyr-223 → Phe mutant is virtually identical to the wild-type enzyme, whereas the Tyr-223 → Ser mutant exhibits 60-fold slower substrate binding and at least 800-fold slower rate of product release relative to wild-type. These data eliminate Tyr-223 as an active-site acid/base catalyst. These results underline the importance of Tyr-223 for substrate binding and exemplify the importance of steric interactions in RgDAAO catalysis.

The enzyme D-amino-acid oxidase (EC 1.4.3.3, DAAO)¹ from the yeast *Rhodotorula gracilis* has been exploited as a potent industrial biocatalyst (for a recent review see Ref. 1) and as a model system for mechanistic studies (2). In contrast to the well known pig kidney DAAO (3), the enzyme from *R. gracilis* is characterized by a comparatively much higher turnover number, good stability under a wide range of reaction conditions, and an active site sufficiently large to accommodate different substrates, even of considerable size (4, 5). Due to these properties, we have utilized the yeast enzyme for the oxidation of cephalosporin C in the two-step formation of 7-aminocephalosporanic acid (6) and for a human gene therapy paradigm that involves oxidant-mediated tumor cell death (7). DAAO catalyzes the oxidation of D-amino acids to α -keto acids and ammonia with concomitant reduction of molecular oxygen to hydrogen peroxide. In the reductive half-reaction, the amino acid substrate reduces the enzyme-bound FAD cofactor producing reduced flavin and the imino acid. In the oxidative half-reaction, the reduced FAD-imino acid complex reacts with molecular oxygen to form oxidized FAD-imino acid. The catalytic

cycle is completed when the imino acid dissociates from the re-oxidized enzyme. Solvolysis of the initial imino acid product rapidly yields the corresponding α -keto acid and ammonia. The enzyme has a broad substrate specificity, utilizing all of the naturally occurring amino acids efficiently, with the only exceptions being aspartate and glutamate (3, 4).

RgDAAO belongs to the large class of flavoprotein oxidases that catalyze the oxidation of amino or α -hydroxy acids. A fundamental question remains within this class of enzymes regarding the mechanism by which a proton and two electrons are transferred from the substrate to the flavin N-5 position during the reductive half-reaction. Substrate oxidation could be accomplished by hydride transfer from the α -carbon to the flavin N-5. Whereas hydride transfer certainly requires stringent orientation of the substrate and flavin cofactor, there is no theoretical argument against it (8). A carbanion mechanism has been proposed in which an enzyme base removes the α -proton (or possibly the amino proton) and so forms a carbanion intermediate (9) (see also Ref. 10 for a recent review). The resulting unstable carbanion would rapidly attack the N-5 locus of the flavin. Subsequent rapid rearrangement would result in reduced flavin and iminopyruvate. The most convincing evidence in favor of a carbanion mechanism is the observation of β -elimination when β -chloroalanine was used as the substrate of pig kidney DAAO (9). Deprotonation of the α -hydrogen of amino acids is highly unfavorable in aqueous solution. Thus, in order for an enzyme to deprotonate the α -proton, it must have some highly specific means of removing the proton and stabilizing the resulting carbanion. Hence, the presence of an enzyme base for α -proton abstraction is essential for the carbanion mechanism.

In order to determine the mechanism of substrate dehydrogenation, we are currently studying the active site of RgDAAO using different experimental approaches. Site-directed mutagenesis of pig kidney DAAO (11) and inspection of its three-dimensional structure (12, 13) have demonstrated that there is no essential base in the vicinity of the flavin N-5. Arg-285, Tyr-238, and Tyr-223 are the only residues conserved in the amino acid sequence of DAAOs from pig, *R. gracilis*, and *Trigonopsis variabilis* (14). Mutagenesis of Tyr-238 is in progress and that of Arg-285 has shown this residue not to be essential for catalysis,² and the study of Tyr-223 has been now completed.

In this paper we report the production and characterization of Y223F and Y223S mutants of RgDAAO. The clarification of the role of the active-site residues of RgDAAO and the resolution of the three-dimensional structure are prerequisite for the identification of the molecular basis of the kinetics, higher

* This work was supported by Grant PRIN 1997–1998 Prot. 9705182517-018 from Italian MURST (to M. S. P.). The costs of publication of this article were defrayed in part by the payment of page charges. This article must therefore be hereby marked “advertisement” in accordance with 18 U.S.C. Section 1734 solely to indicate this fact.

‡ Present address: Dept. of Chemistry, University of Utah, Salt Lake City, UT 84112.

§ To whom correspondence should be addressed: Dept. di Biologia Strutturale e Funzionale, Università degli Studi dell’Insubria, via J.H. Dunant 3, 21100 Varese, Italy. Tel.: 332-421506; Fax: 332-421500; E-mail: polleg@imiucca.csi.unimi.it.

¹ The abbreviations used are: DAAO, D-amino-acid oxidase (EC 1.4.3.3); RgDAAO, *R. gracilis* D-amino-acid oxidase; XO, xanthine oxidase; IA, imino acid; CF₃-alanine, 3,3,3-trifluoro-DL-alanine.

² L. Pollegioni, personal communication.

catalytic efficiency, substrate specificity, and flavin binding properties that differentiate RgDAAO from the mammalian enzyme. Site-directed mutagenesis has a second application with regard to the use of RgDAAO as a biocatalyst (for a review see Ref. 1). Engineering of the substrate specificity and affinity of this enzyme could have relevant applications both in bioconversions and in gene therapy (the latter requiring an enzyme form with higher affinity for the D-amino acid and oxygen).

EXPERIMENTAL PROCEDURES

Reagents—Restriction enzymes and T4 DNA ligase were from Roche Molecular Biochemicals. FlexiPrep[®] Kit and Sephaglass BandPrep[®] Kit were from Amersham Pharmacia Biotech. Site-directed mutagenesis reactions were made using the Altered Sites[®] II Kit (Promega). CF₃-alanine was from ABCR GmbH. D-Amino acids, xanthine, xanthine oxidase, and all other compounds were purchased from Sigma. 5-Deazaflavin was a generous gift of Dr. Sandro Ghisla (University of Konstanz, Germany). All experiments were performed in 50 mM sodium pyrophosphate, pH 8.5, 1% glycerol, 0.3 mM EDTA, and 0.5 mM 2-mercaptoethanol and at 25 °C, except where stated otherwise.

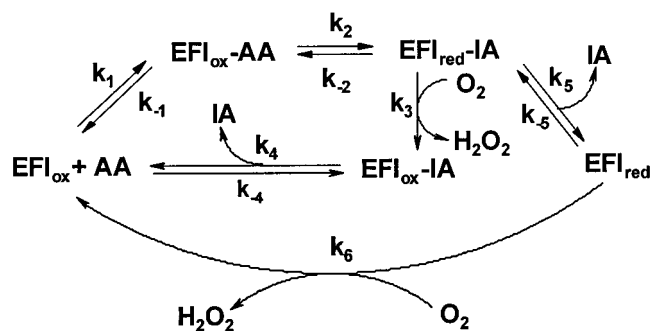
Site-directed Mutagenesis—The RgDAAO-Y223F mutant was generated by site-directed mutagenesis using the Altered Sites[®] II Kit; the cDNA coding for the wild-type RgDAAO was subcloned in the *EcoRI* pALTER-1[®] vector. The plasmid was then purified as single strand DNA by phage infection (as described in the Promega protocol) and used as a template for the *in vitro* mutagenesis reactions. The mutant was generated using a dual primer method to introduce simultaneously a site-directed mutation (Y223F2, CCCGCTTCTCCCGCATTCATCATT-CCCCGA, the codon for phenylalanine is underlined) and ampicillin resistance. *In vitro* mutagenesis reaction products were used to transform competent *Escherichia coli* ES1301 mutS cells and finally *E. coli* JM109 cells (15). Successful mutagenesis was screened for the insertion of a new *BsmI* site (GAAT(G/C)N) by restriction analysis and confirmed by DNA sequencing.

The Y223S mutant was generated by mutagenic polymerase chain reaction. The plasmid pCRII-DAAOwt carrying the wild-type RgDAAO cDNA (16) was used as the template in the amplification reactions. The DNA was amplified using the Y223S upstream primer (CAATCCGCG-GGCAAACCGTCTCGTCAAGTCCCATTGCAAGCGATGCACGATG-GACTCGTCCGACCCCGCTTCTCCCGCTCCATCATT, the codon for serine is underlined), which carried the punctiform mutation, and the 3' downstream primer (CTTGTAGATGCCGCAATACAG). The latter was designed to anneal after the poly(A) tail of the cDNA. The amplification product was cloned into the pCRII vector (Invitrogen) and sequenced to confirm the presence of the desired mutation. A cassette (*SacII* and *HindIII*) containing the mutant Y223S was exchanged with the corresponding fragment of pKK-DAAO plasmid (16). The complete RgDAAO-Y223S and RgDAAO-Y223F cDNAs were subcloned into the *EcoRI* site of the pT7.7A expression vector (U. S. Biochemical Corp.), and the mutated region was sequenced again. The new expression plasmids were designated pT7-Y223S and pT7-Y223F and were used to transform *E. coli* BL21(DE3) and BL21(DE3)pLysS cells (Novagen Inc.).

Activity Assay and Gel Electrophoresis—During purification, DAAO activity was assayed with an oxygen electrode at pH 8.5 and 25 °C with 28 mM D-alanine as substrate (4). One DAAO unit is defined as the amount of enzyme that converts 1 μmol of D-alanine per min, at 25 °C. Analytical SDS-polyacrylamide gel electrophoresis was carried out as described by Laemmli (17).

Enzyme Expression and Purification—The Y223S and Y223F RgDAAO mutants were expressed in *E. coli* using the recently developed pT7-DAAO expression system in BL21(DE3)pLysS *E. coli* cells (18). A fermentor (PPS-3, Bioindustrie Mantovane) containing 10 liters of Luria Bertani medium, 100 μg/ml ampicillin, and 34 μg/ml chloramphenicol was inoculated with 500 ml of an overnight culture of pT7-Y223S or pT7-Y223F expression system ($A_{600} = 3.2$). Cells were grown at 37 °C for 2.5 h ($A_{600} = 1.0$) and then induced with 0.6 mM isopropyl-D-thiogalactopyranoside (final concentration). Induced cells were grown at 30 °C for 21 h and then harvested by centrifugation and stored at -20 °C. Purification of both Y223F and Y223S mutants was performed by the identical procedure as for recombinant wild-type RgDAAO (18).

Spectral Experiments—The extinction coefficients for the mutant DAAO enzymes were determined by measuring the change in absorbance after release of the flavin. The enzymes were heat-denatured by boiling for 5 min in the dark; an extinction coefficient of 11,300 M⁻¹ cm⁻¹ at 450 nm for free FAD was used.



SCHEME 1. Kinetic scheme of RgDAAO. The inner loop shows the ternary complex mechanism, and the outer loop depicts the ping-pong mechanism.

Photoreduction and Stabilization of Flavin Semiquinone—An anaerobic cuvette containing 7.5 μM enzyme, 5 mM EDTA, and 0.5 μM 5-deazaflavin was made anaerobic and photoreduced with a 250-watt lamp, with the cuvette immersed in a 0 °C water bath. Progress of the reaction was followed spectrophotometrically. When the semiquinone peak at 370 nm reached its maximal value, 15 min irradiation, 5 μM benzyl viologen was added from a side arm of the cuvette, and the absorbance changes were followed for up to 24 h at 15 °C.

Redox Potentials—Redox potentials for the EFl_{ox}/EFl_{seq} and EFl_{seq}/EFl_{red} couples (where EFl_{ox} is oxidized enzyme; EFl_{seq} is enzyme flavin semiquinone; and E_{red} and EFl_{red} , reduced enzymes) of Y223F and Y223S mutants were determined by the method of dye equilibration (19) using the xanthine/xanthine oxidase (XO) reduction system, at 15 °C (20). An anaerobic cuvette containing 7 μM enzyme, 0.2 mM xanthine, 5 μM benzyl viologen, and 1–10 μM of the appropriate dye was purged of oxygen, and the reaction was initiated by addition of 10 nM XO. The reaction was measured spectrophotometrically until completion, typically 3–4 h. Data were analyzed as described by Minnaert (19). The amount of oxidized and reduced dye was determined at a wavelength where the enzyme has no absorbance (>550 nm), and the amount of oxidized and reduced enzyme was determined at an isobestic point for the dye or by subtraction of the dye's contribution in the 400–470 nm region.

Ligand Binding—Dissociation constants for ligands were measured spectrophotometrically by addition of small volumes (1–10 μl) of concentrated stock solutions to samples containing 1 ml of 7–11 μM enzyme, at 15 °C. The change in absorbance upon adding ligand was plotted as a function of ligand concentration, after correction for any volume change. Wavelengths used for the ligands are 497 nm for sodium benzoate and sodium crotonate, 456 nm for sodium sulfite, 540 nm for sodium anthranilate, and 485 nm for CF₃-alanine. Specificity for L-amino acids was checked by following the change in the absorbance spectrum after anaerobic addition of the amino acid to the enzyme solution.

Stopped-flow Measurements—The experiments were performed at 25 °C in a thermostatted stopped-flow spectrophotometer with a 2-cm path length cell and that is equipped with a diode array detector as described previously (2). Steady-state kinetic analysis was performed by the method of enzyme-monitored turnover by mixing air-saturated enzyme, 10 μM (final concentration), with air-saturated solutions of D-alanine at 25 °C. Traces at 456 nm were analyzed as described previously (21) using the Kaleidagraph program (Synergy Software). The ternary complex mechanism shown in the inner loop of Scheme 1 can be described using the conventions of Dalziel (22) as shown in Equations 1 and 2.

$$e/v = \Phi_0 + \Phi_{AA}/[AA] + \Phi_{O_2}/[O_2] + \Phi_{AAO_2}/[AA][O_2] \quad (\text{Eq. 1})$$

where (AA indicates D-amino acid)

$$k_{cat} = 1/\Phi_0; K_{m(D-Ala)} = \Phi_{AA}/\Phi_0; K_{m,O_2} = \Phi_{O_2}/\Phi_0$$

$$\frac{e_t}{v} = \frac{k_2 + k_4}{k_2 \cdot k_4} + \frac{k_{-1} + k_2}{k_1 \cdot k_2 [AA]} + \frac{k_2 + k_{-2}}{k_2 \cdot k_3 [O_2]} + \frac{k_{-1} + k_{-2}}{k_1 \cdot k_2 \cdot k_3 [AA][O_2]} \quad (\text{Eq. 2})$$

For reductive half-reaction experiments, the stopped-flow instrument was made anaerobic by overnight equilibration with concentrated sodium dithionite solutions. Prior to use, the instrument was well rinsed with nitrogen-bubbled buffer to remove the dithionite. The reaction was followed by taking spectra with a diode array detector from 3 ms until

completion. Reaction rates were calculated by extracting traces at individual wavelengths (456 and 530 nm) and fitting them to a sum of exponentials equation using Program A (developed in the laboratory of Dr. David P. Ballou at the University of Michigan). Subsequent analysis of k_{obs} values determined with Program A were fit by non-linear least means squares procedures with Kaleidagraph. Unlike the wild-type RgDAAO, formation of the $E_{\text{red}}\text{-IA}$ complex for study of the oxidative half-reaction could not be obtained by addition of stoichiometric D-alanine in the presence of pyruvate and ammonia. Instead the xanthine/XO system was used. A tonometer with an anaerobic cuvette was loaded with a 4.5-ml solution containing 16–18 μM mutant DAAO in buffer A (50 mM sodium pyrophosphate, pH 8.5, 1% glycerol, 20 mM sodium pyruvate and 0.4 M ammonium chloride), 84 nM XO, 4 μM methyl viologen, and 9 μM cresyl violet (for Y223F-DAAO) or 4 μM benzyl viologen and 1.3 μM indigo disulfonate (for Y223S-DAAO). The sample was made anaerobic, and enzyme reduction was initiated by addition of 400 μM xanthine. The sample required about 2 h for full reduction. The pre-reduced enzyme was loaded onto the stopped-flow instrument under anaerobic conditions. It was then reacted with solutions of buffer A that had been bubbled at 25 °C with air, commercially available N_2/O_2 mixtures (90/10, 50/50), or pure oxygen. Data were collected and analyzed as described for the reductive half-reaction.

RESULTS

Enzyme Expression and Purification—The pT7-Y223F and pT7-Y223S plasmids were used to transform BL21(DE3) and BL21(DE3)pLysS *E. coli* cells, and the induction conditions were investigated with both expression systems by Western blot analysis and DAAO activity assay. Analogously to the wild-type RgDAAO (18), the highest level of DAAO expression and DAAO specific activity was obtained when the BL21(DE3) *E. coli* carried the pLysS plasmid (8.7 units/mg protein and 0.07 units/mg protein for the Y223F and Y223S mutants, respectively), inducing the cells with 0.6 mM isopropyl-D-thiogalactopyranoside at saturation ($A_{600} \geq 2.0$) and growing at 30 °C for additional 3–24 h. Typically 45–75 mg of pure enzyme was isolated from 10 liters of bacterial growth of Y223S or Y223F, compared with 180 mg for wild-type DAAO (18).

Spectral Properties—Both Y223F and Y223S mutations yielded well behaved enzymes that retained their FAD prosthetic group and that were stable when stored at –20 °C for several months. Visible spectra of Y223F and Y223S enzymes are shown in Fig. 1 in comparison to the wild-type RgDAAO. Both mutants, in their oxidized state, show an extinction coefficient at 455 nm of $12750 \text{ M}^{-1} \text{ cm}^{-1}$ and a ratio of $A_{274}/A_{455} \approx 8.7$. Anaerobic addition of an excess of D-alanine (Fig. 1) resulted in instantaneous enzyme reduction of both mutant DAAOs, with a spectrum like that of the wild type. The amount of semiquinone form stabilized by each mutant was determined by anaerobic photoreduction (23) until the spectrum of the flavin semiquinone ($EF1_{\text{seq}}$) reached a maximum (Fig. 1); this species represents near-complete formation of $EF1_{\text{seq}}$ ($\approx 95\%$). The maximal semiquinone formed by photoreduction is a kinetically stabilized species. Anaerobic addition of benzyl viologen resulted in dismutation of $EF1_{\text{seq}}$ to the oxidized and reduced forms over a period of 15 min with the end point containing the thermodynamically stabilized amount of semiquinone. Y223F and Y223S enzymes stabilized 60 and 63%, respectively, of the red, anionic flavin semiquinone, compared with 65% for the wild type (Table I). Stabilization of the anionic semiquinone is typical for D-amino-acid oxidases and for the family of flavoprotein oxidases (24).

Redox Potentials—In order to assess changes in the thermodynamic properties of the flavin center caused by mutation at Tyr-223, the redox potentials of the enzymes were measured by the dye equilibration method of Minnaert (19) using the xanthine/XO reduction system (20). A representative experiment is shown in Fig. 2 in which the potential of the $EF1_{\text{ox}}/EF1_{\text{seq}}$ couple of Y223F was measured in reference to methylene blue. A replot (Fig. 2, inset) of the log (oxidized/reduced) methylene

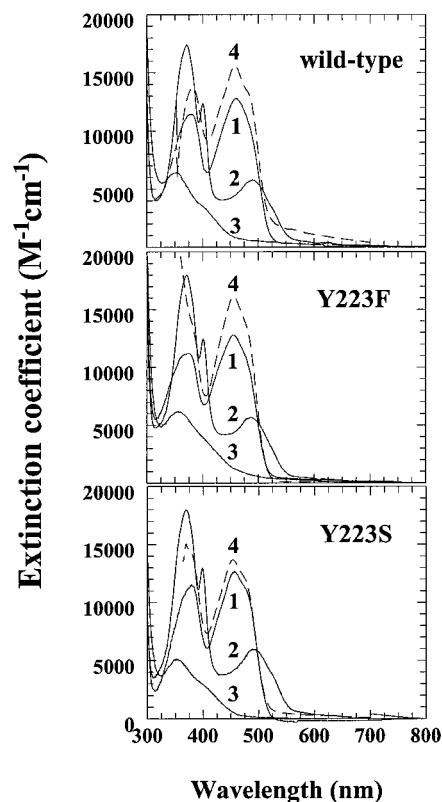


FIG. 1. Spectral properties of wild-type, Y223F, and Y223S D-amino-acid oxidases. 1, oxidized enzyme in 50 mM sodium pyrophosphate buffer, pH 8.5, containing 1% glycerol, 0.3 mM EDTA, and 5 mM 2-mercaptoethanol, at 15 °C; 2, semiquinone form generated by photoirradiation; 3, fully reduced enzyme from anaerobic reaction with 5 mM D-alanine; 4, $E_{\text{ox}}\text{-IA}$ complex obtained in the presence of 400 mM ammonium chloride and 200 mM pyruvate.

TABLE I
Semiquinone formation and stabilization and redox potentials of wild-type, Y223F, and Y223S D-amino-acid oxidases

The semiquinone form of DAAO was achieved by anaerobic photoreduction, and the percentage of the thermodynamically stabilized form was measured after equilibration with benzyl viologen.

	Semiquinone measured		E^0_1	E^0_2	E_m
	Kinetically stabilized	Thermodynamically stabilized			
		%	mV		
Wild-type	≥ 95	65	–60 ^a	–200 ^b	–130
Y223S	≥ 95	60	–36 ^a	–170 ^b	–103
Y223F	90	63	–59 ^a	–203 ^c	–131

^a The redox potentials were measured at pH 8.5 and 15 °C using methylene blue (–29 mV) as redox standards, and xanthine/xanthine oxidase as the source of reducing equivalents (20).

^b The redox potentials were measured at pH 8.5 and 15 °C using indigo disulfonate (–159 mV) as redox standards, and xanthine/xanthine oxidase as the source of reducing equivalents (20).

^c The redox potentials were measured at pH 8.5 and 15 °C using cresyl violet (–197 mV) as redox standards, and xanthine/xanthine oxidase as the source of reducing equivalents (20).

blue as a function of log (oxidized/semiquinone) flavin species gives the potential of the $EF1_{\text{ox}}/EF1_{\text{seq}}$ couple when the potential of the indicator is known (19). The line plotted in the inset of Fig. 2 has a slope of 1.96 in excellent agreement with the theoretical value of 2 expected for a 2- to 1-electron couple. Decreasing the concentration of XO, and thus slowing the rate at which the reaction proceeds, had no effect on the potentials measured. In the case of Y223F, the potentials of both couples are identical to those of the wild-type enzyme, whereas the Y223S mutant has potentials each about 25 mV more positive

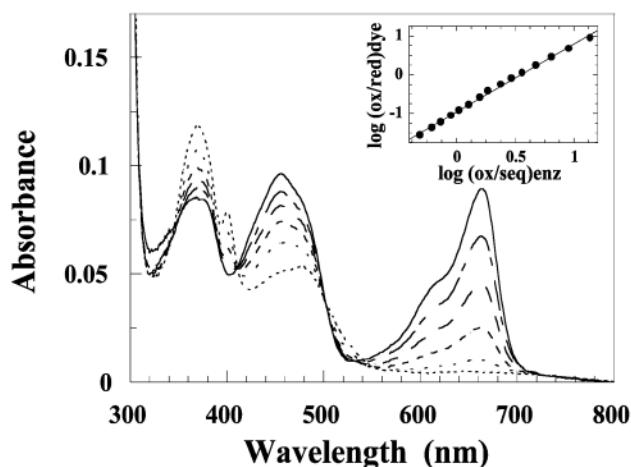


FIG. 2. Determination of the redox potentials of Y223F mutant. Selected spectra obtained during the course of the anaerobic reduction of $7.2 \mu\text{M}$ Y223F DAAO in 50 mM sodium pyrophosphate buffer, pH 8.5, containing 1% glycerol, 0.3 mM EDTA, and 5 mM 2-mercaptoethanol, in the presence of 160 μM xanthine and 0.9 μM methylene blue ($E_m = -29$ mV) and 5 μM benzyl viologen. —, before addition of 10 nM xanthine oxidase; ---, 30 min; - - -, 45 min; ···, 60 min; - · - ·, 80 min; and ····, 120 min after addition of xanthine oxidase. Inset, Nernst plot according to Minnaert (19), $n = 1.96$.

than the wild type (Table I). This change in the Y223S potentials should have little influence on catalysis because the FAD midpoint potential of -103 mV makes enzyme reduction by D-alanine (rate-limiting for wild-type enzyme) slightly more thermodynamically favorable; retardation of the oxidative half-reaction is not an issue because the $\text{O}_2/\text{H}_2\text{O}_2$ couple is so much more positive (+300 mV at pH 7) than the FAD/FADH₂ couple. Y223F and Y223S mutations had no significant effect on the redox potentials of the enzyme-bound FAD.

Ligand Binding—Dissociation constants for several ligands were measured in order to determine the contribution of residue Tyr-223 to substrate binding. In each case, binding was measured by the perturbation of the visible spectrum of the FAD upon formation of the bound complex (not shown), and with all the compounds tested and for both Y223F and Y223S mutants, the spectral modifications were identical to those observed for the binding to the wild-type DAAO. Only modest effects of 5–7-fold weakening in binding was observed for both mutants with the ligands CF₃-alanine, benzoate and sulfite (Table II). CF₃-alanine is not a substrate for the enzyme, as determined by anaerobic addition of the compound to the enzyme (not shown).

The higher K_d for sulfite parallels the results obtained with CF₃-alanine and is somewhat surprising due to the modest changes in redox potentials of the mutants (see Table I). Binding of crotonate and anthranilate to the mutants was more substantially reduced (up to 23-fold higher K_d for anthranilate observed with the Y223F-DAAO), but these compounds have little structural resemblance to amino acid substrates. Both mutants maintain the stereospecificity of the wild-type RgDAAO; they are not reduced by L-alanine and L-valine under anaerobic conditions.

Steady-state Kinetics—The ability of the Y223F and Y223S mutants to catalyze D-alanine/oxygen catalysis was measured by enzyme-monitored turnover. Air-saturated solutions of enzyme and of D-alanine were mixed in the stopped-flow spectrophotometer, and the absorbance spectra were recorded continuously in the 350–650 nm wavelength range at 25 °C. Following the absorbance at 456 nm, an initial rapid decrease of the oxidized flavin absorption was observed, followed by a steady-state phase, and then by a further decrease to reach the

TABLE II
Binding of aromatic and aliphatic competitive inhibitors, CF₃-D-alanine, and sulfite to wild-type, Y223F, and Y223S D-amino acid oxidases

All measurements were made at pH 8.5 and 15 °C.

Compound	K_d		
	Wild type	Y223S	Y223F
		<i>mM</i>	
Benzoate	0.9	5.0	6.4
Anthranilate	1.9	2.5	44
Crotonate	0.4	7.0	5.3
CF ₃ -D-alanine	6.7	29	36
Sulfite	0.12	0.66	0.85

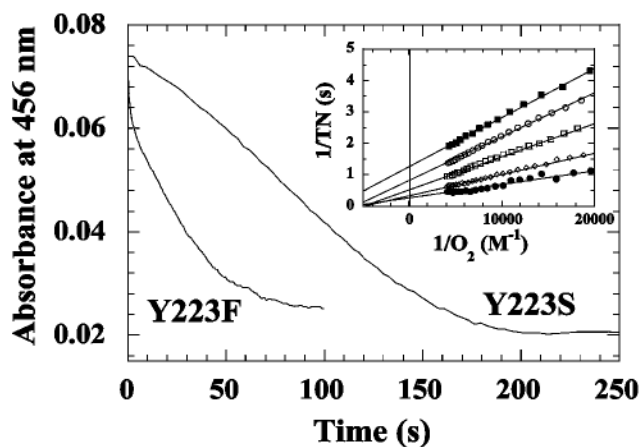


FIG. 3. Time courses of turnover of Y223F and Y223S mutant RgDAAOs followed in the stopped-flow spectrophotometer. The changes in absorbance were monitored at 456 nm after mixing 5.5 μM mutant enzyme with 1.25 mM D-alanine (all final concentrations). For the sake of clarity, the time scale for Y223F was multiplied by a factor of 20. Inset, Lineweaver-Burk plot of the data determined from the enzyme-monitored turnover traces of Y223S in the main graph, obtained at the following D-alanine concentrations: 1.25 mM (■), 2.5 mM (○), 5.0 mM (□), 12.5 mM (◇), and 30 mM (●).

final reduced state. This confirms that both the Y223F and Y223S mutants are competent catalysts (Fig. 3). With Y223F and Y223S mutants, as well as for the wild-type DAAO, the enzyme is largely present in the oxidized form during turnover. This indicates that the overall process of reoxidation of reduced DAAO with oxygen is faster than the reductive half-reaction. Although the steady-state phase is quite short, the Lineweaver-Burk plots of D-alanine/oxygen turnover (as well as with D-valine) show a set of converging lines with both DAAO mutants (shown only for Y223S with D-alanine, inset of Fig. 3), consistent with a ternary complex mechanism. For wild-type DAAO with D-alanine as substrate, a parallel line pattern in the secondary plots was instead found (5), consistent with a limiting case of a ternary complex mechanism where some specific rate constants (*i.e.* k_{-2} , the reverse of the reduction rate) are sufficiently small. For Y223F, k_{cat} is only reduced by about one-third, and the K_m for D-alanine and O_2 are essentially unchanged. For Y223S, k_{cat} is reduced about 80-fold, K_m for D-alanine is increased 2-fold, and K_m for oxygen is decreased 15-fold (Table III). The drastic change in kinetic parameters of Y223S with D-alanine was confirmed by studying the reaction of Y223S using D-valine as substrate (Table III).

Reductive Half-reaction—The reductive half-reaction of Y223F and of Y223S with D-alanine was measured to assess the influence of each mutation on individual rate constants. An anaerobic solution of each enzyme was mixed anaerobically with solutions containing varying concentrations of D-alanine, such that a pseudo-first-order condition was maintained with

TABLE III

Comparison of the steady-state coefficients for wild-type, Y223F, and Y223S D-amino-acid oxidases with D-alanine and D-valine as substrates, at pH 8.5 and 25 °C

All measurements were made in 50 mM sodium pyrophosphate, pH 8.5, 1% glycerol, 0.3 mM EDTA, and 0.5 mM 2-mercaptoethanol.

		D-Alanine	D-Valine
k_{cat} (s^{-1})	Wild type ^a	350 ($\approx k_2$)	29
	Y223S	4.2 ($\approx k_4$)	2.8
	Y223F	210	Not determined
$1/\Phi_{\text{AA}}$ ($\text{M}^{-1} \text{s}^{-1}$)	Wild type ^a	1.7×10^5	4.4×10^5
	Y223S	7.3×10^2	46
	Y223F	1.2×10^5	Not determined
$1/\Phi_{\text{O}_2}$ ($\text{M}^{-1} \text{s}^{-1}$)	Wild type ^a	1.5×10^5	2.2×10^6
	Y223S	0.28×10^5	4.7×10^3
	Y223F	4.4×10^5	Not determined
$1/\Phi_{\text{AAO}_2}$ ($\text{M}^{-2} \text{s}^{-1}$)	Wild type ^a	≈ 0	≈ 0
	Y223S	2.8×10^6	3.8×10^6
	Y223F	2.8×10^8	Not determined
K_{AA} (mM)	Wild type ^a	2.6	3.9
	Y223S	6.0	61
	Y223F	2.2	Not determined
K_{O_2} (mM)	Wild type ^a	2.3	0.8
	Y223S	0.15	0.32
	Y223F	1.4	Not determined

^a Wild-type enzyme data are from Pollegioni *et al.* (5), determined in 60 mM sodium pyrophosphate buffer, pH 8.5, containing 1.5% glycerol, 0.3 mM EDTA, and 0.75 mM 2-mercaptoethanol, at 25 °C.

respect to the substrate concentration. In the absence of oxygen, the enzyme undergoes only one-half of a normal catalytic cycle; the substrate binds, reduces the enzyme, and the product dissociates (steps designated by k_1/k_{-1} , k_2/k_{-2} , and k_5/k_{-5} in Scheme 1). The same species are observed in the reductive half-reaction of both mutants. Upon mixing with D-alanine, the oxidized enzyme is rapidly converted to the $E_{\text{red}} \cdot \text{IA}$ complex, as is shown in the case of Y223F in Fig. 4. These spectra show a very small amount of semiquinone formed photochemically due to the high intensity lamp of the stopped-flow instrument. There is no observed spectral change associated with formation of the oxidized enzyme-D-alanine complex. Formation of the spectral intermediate, phase 1, involves a large extinction decrease at 456 nm and a small extinction increase at 530 nm (Fig. 4), consistent with formation of a $E_{\text{red}} \cdot \text{iminopyruvate}$ charge-transfer complex (25). Decay of the spectral intermediate, phase 2, results in a spectrum consistent with the presence of free, reduced enzyme (Fig. 4) (5). Reaction traces at 456 and 530 nm demonstrate the time dependence of the spectral changes (Fig. 4, inset). By using Program A, traces were fit to a two exponential consecutive Marquardt algorithm such that the first exponential corresponds to enzyme reduction (k_2/k_{-2}) and the second exponential corresponds to product dissociation (k_5/k_{-5}).

The Y223F mutant has only a slightly hyperbolic dependence of the observed reduction rate, k_{obs1} , as a function of D-alanine concentration. The k_{obs} values near saturation are so fast as to be at the detection limit of the stopped-flow instrument (Fig. 5). A double-reciprocal plot of these data does clearly indicate a positive y intercept (not shown). Hyperbolic behavior on the direct plot has been analytically demonstrated by Strickland and colleagues (26) to describe a first-order reaction of a binary complex, k_2/k_{-2} , that follows a second-order complex formation, k_1/k_{-1} . By using such a model, the reduction rate, k_2 , for Y223F is $1,220 \pm 400 \text{ s}^{-1}$, and the $K_{d(\text{app})}$ is 23 mM (Table IV). Since the data are best fit with a rectangular hyperbola which intersects the origin, these data indicate that the reduction step is essentially irreversible ($k_{-2} = 0$). Numerically, the value of $K_{d(\text{app})}$ is equal to $(k_{-1} + k_2)/k_1$ (26). For wild-type RgDAAO, it

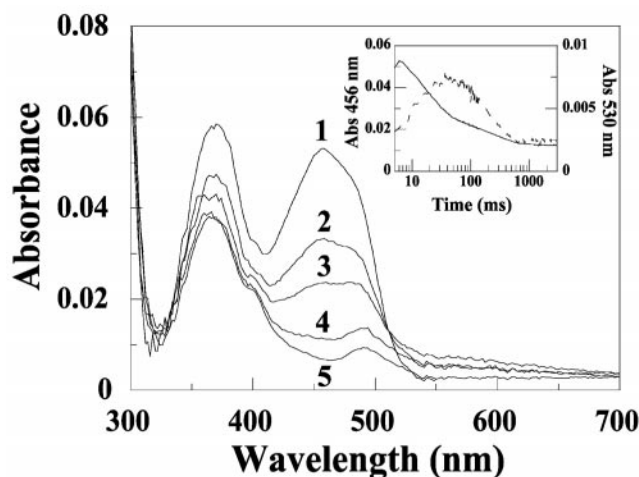


FIG. 4. Time course of anaerobic reduction of Y223F DAAO using D-alanine, followed in the stopped-flow instrument. Anaerobic Y223F DAAO ($7.89 \mu\text{M}$) was anaerobically reacted with 2.5 mM D-alanine, at pH 8.5 and 25 °C. 1, 50 ms; 2, 100 ms; 3, 160 ms; 4, 1 s; and 5, 1.94 ms after mixing. Inset, time course of anaerobic reduction of the same reaction followed at two different wavelengths: at 456 nm (—) the traces reflect the conversion of oxidized to fully reduced enzyme, at 530 nm (---) the formation and decay of reduced enzyme-IA complex.

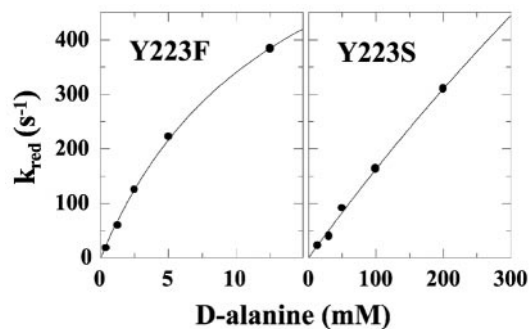


FIG. 5. Dependence of the observed rate for the first phase (k_{obs1}) of the anaerobic reduction of Y223F and Y223S on the concentration of D-alanine. Conditions as reported in the legend of Fig. 4.

has been shown that D-alanine is a “sticky” substrate ($k_2 \gg k_{-1}$), and so $K_{d(\text{app})} = k_2/k_1$. Thus the increase in $K_{d(\text{app})}$ for Y223F possibly reflects the increase in k_2 rather than a change in binding. Product dissociation from Y223F (k_5 , the second phase) has a substrate concentration-independent value of 7.7 s^{-1} , a small increase over the wild-type enzyme. Although our estimate of k_2 is greater than k_{cat} and would suggest a change in the slow step in catalysis, it is more likely that k_2 is still (partially) rate-limiting for Y223F. The 6-fold difference between k_2 and k_{cat} could be explained by the uncertainty inherent in measuring values this fast or in a decrease in k_4 , the rate for iminopyruvate dissociation from the reoxidized enzyme form. By using the measured values of k_{cat} and k_2 , a lower limit for k_4 of 254 s^{-1} can be estimated (see Equation 1). Because k_5 ($= 7.7 \text{ s}^{-1}$) is very much slower than k_{cat} ($= 210 \text{ s}^{-1}$), k_5 clearly does not lie within the catalytic cycle, and the steady-state mechanism must be entirely ternary complex.

For the reductive half-reaction of Y223S, a quasi-linear dependence of k_{obs} as a function of D-alanine concentration (Fig. 5) is observed up to the solubility limit of D-alanine, indicating that the $K_{d(\text{app})}$ for D-alanine is greatly increased for this mutant. This is a limiting case of a second-order reaction with D-alanine ($k = 1.5 \times 10^3 \text{ M}^{-1} \text{ s}^{-1}$), when the binding of the substrate ($k_1 \cdot [\text{S}]$) is slower than flavin reduction (k_2). By using the treatment previously described for a first-order reaction of

TABLE IV

Reductive half-reaction specific rate constants obtained from stopped-flow experiments of wild-type, Y223F, and Y223S DAAOs with D-alanine and D-valine as substrates, at pH 8.5 and 25 °C

The values were determined using a model of a second-order binding reaction followed by a first-order chemical step, although the reaction of Y223S with D-alanine can be considered a limiting case under second-order kinetic conditions. The apparent K_d was obtained from the slope divided by the intercept in double-reciprocal plots (not shown) of the measured rates for the first rapid phase of enzyme reduction ($k_{\text{obs}1}$) versus substrate concentration.

	D-Alanine			D-Valine				
	k_2	$\frac{K_{d(\text{app})}}{=(k_{-1} + k_2)/k_1}$	$\frac{k_2 K_{d(\text{app})}}{\approx k_1}$	k_5	k_2	$\frac{K_{d(\text{app})}}{=(k_{-1} + k_2)/k_1}$	$\frac{k_2 K_{d(\text{app})}}{\approx k_1}$	k_5
	s^{-1}	mM	$mM^{-1} s^{-1}$	s^{-1}	s^{-1}	mM	$mM^{-1} s^{-1}$	s^{-1}
Wild type ^a	340	2.8	120	2.8	30	3.8	7.8	1.2
Y223S	1400	710	1.9	35	21	560	0.037	^b
Y223F	1220	23	54	7.7		Not determined		

^a Wild-type enzyme data are from Ref. 5, determined in 60 mM sodium pyrophosphate buffer, pH 8.5, containing 1.5% glycerol, 0.3 mM EDTA, and 0.75 mM 2-mercaptoethanol, at 25 °C.

^b Essentially monophasic.

a binary complex, a value of $k_2 \geq 1,400 \pm 200 s^{-1}$ was estimated by fitting a double-reciprocal plot of these data and clearly involves a large extrapolation. Measurement of a k_{obs} value of $310 s^{-1}$ at 200 mM D-alanine, compared with a limiting value of k_2 for wild-type enzyme of $335 s^{-1}$ at saturating substrate (5), does clearly indicate that enzyme reduction is not decreased in the Y223S mutant, but may be increased. The estimated value of $K_{d(\text{app})} = 710 mM$ is 250-fold greater for Y223S than for wild-type RgDAAO. Since k_2 is probably only about 5 times increased over the wild type, this clearly involves a significant decrease in k_1 . The second phase in reduction, k_5 , has a D-alanine concentration-independent value of $35 s^{-1}$ (a value 8-fold greater than k_{cat} , Table III and IV). Based on Equation 3

$$k_{\text{cat}} = k_2 \cdot k_5 / (k_2 + k_5 + k_{-2}) \quad (\text{Eq. 3})$$

for a ping-pong mechanism (the outer loop in Scheme 1), and by using $k_2 = 1,400 s^{-1}$, $k_{-2} \approx 0$, and $k_5 = 35 s^{-1}$, Y223S turnover is at most 13% ping pong, thus supporting a ternary complex mechanism (Equation 4, the inner loop of Scheme 1) as follows:

$$k_{\text{cat}} = k_2 \cdot k_4 / (k_2 + k_4) \quad (\text{Eq. 4})$$

Since k_2 for Y223S is at least 330-fold greater than k_{cat} , there must be a significant change in k_4 , in the oxidative half-reaction (a value of about $4.2 s^{-1}$ can be estimated with Equation 4). To support further the effect of the mutation on the binding of substrate, the reductive half-reaction of Y223S mutant with D-valine was also investigated. The plot of k_{obs} versus D-valine concentration gave a hyperbolic curve (data not shown). The rate of reduction is only slightly affected by the substitution, whereas the apparent K_d showed an approximately 150-fold increase due to a large decrease in k_1 (Table IV). Interestingly, the course of the reaction at 456 nm is essentially monophasic, probably because $k_2 \leq k_5$.

Oxidative Half-reaction—To assess further changes in reactivity of the mutants, and because reduction of Y223S is much faster than k_{cat} , the oxidative half-reactions of both mutants were investigated. During catalysis of wild-type RgDAAO, the $E_{\text{red}}\cdot\text{IA}$ complex reacts with oxygen to form the $E_{\text{ox}}\cdot\text{IA}$ complex (where E_{ox} is oxidized enzyme) (k_3 of Scheme 1). A catalytic cycle is completed with the subsequent dissociation of iminopyruvate (5). Preparation of the $E_{\text{red}}\cdot\text{IA}$ complex for measurement of the oxidative half-reaction is difficult due to the spontaneous solvolysis of iminopyruvate to ammonia and pyruvate. In order to provide sufficient iminopyruvate to study the oxidation of the reduced, binary complex, the equilibrium position of the solvolysis reaction was shifted by performing reactions in the presence of 0.4 M ammonium chloride and 20 mM sodium pyruvate. Although this procedure functioned well for wild-type RgDAAO, it is possible that the reduced, mutant enzymes have

lower affinity for the product and that the reaction may not involve fully bound, reduced enzyme. With both Y223F and Y223S mutants, the substrate reduction of anaerobic oxidized enzyme in the presence of pyruvate and ammonia failed to produce an enzyme form having spectral properties resembling those of the $E_{\text{red}}\cdot\text{IA}$ complex. For this reason Y223F and Y223S DAAOs were reduced in the presence of pyruvate and ammonia using the xanthine/XO reduction method, as performed for the determination of redox potentials (see above). The reduced, iminopyruvate-bound enzyme was reacted in the stopped-flow spectrophotometer with buffer solutions equilibrated with different concentrations of oxygen. Reaction traces at 456 nm were monophasic (not shown), and spectra during the reaction (not shown) indicate that reduced enzyme is converted to oxidized without any intermediate species. The plots of k_{obs} versus oxygen concentration (not shown) are linear and intersect at the origin, indicating that the reactions are second-order and irreversible with rate constants of $k_3 = 6.3 \times 10^4 M^{-1} s^{-1}$ for Y223F and $1.4 \times 10^5 M^{-1} s^{-1}$ for Y223S, comparable to the reoxidation rate of the wild-type enzyme (Table V) (5).

These experiments indicate that both Tyr-223 mutants react as rapidly with oxygen as the wild-type enzyme. However, there is no measurable spectral change associated with k_4 , and it is thus not observed. The binding of iminopyruvate to the oxidized form of DAAO was investigated by static titration using increasing amounts of pyruvate in the presence of 400 mM ammonia (to shift the equilibrium toward IA production). In all cases, the addition of pyruvate to wild-type and mutant DAAOs results in an increase in absorbance at 455 and 560 nm, but with a different extent in the three cases (Table V and Fig. 1). Apparent K_d values are reported because the true concentration of iminopyruvate in the solution is unknown. These K_d values therefore represent minimal values. Comparison of the change in apparent K_d between enzymes is completely valid.

DISCUSSION

The expression system constructed to maximize the production in *E. coli* of wild-type RgDAAO was also used successfully to express mutant DAAOs. The enzymes can be purified to homogeneity with a good yield ($\geq 20\%$), similar to wild-type RgDAAO (18). Spectral properties of the oxidized, semiquinone, and reduced forms of the Y223F and Y223S mutants are essentially the same as wild-type DAAO (Fig. 1). The flavin redox potentials of Y223F are indistinguishable from the wild-type enzyme, whereas the midpoint (and each half-potential) of Y223S is 30 mV more positive than wild-type (Table I). A change in 30 mV corresponds to $0.7 \text{ kcal mol}^{-1}$, a difference significantly smaller than the energy of a single hydrogen bond. The ligand-binding experiments demonstrate that the overall substrate-binding pocket remains intact, since both mu-

TABLE V

Rate constants from the oxidative half-reaction and dissociation constants for product binding for wild-type, Y223S, and Y223F DAAOs

	Oxidative half-reaction ^a		Iminopyruvate binding ^b		
	k_3	k_6	$K_{d(\text{app})}$	$\Delta\epsilon_{455 \text{ nm}}$	$\Delta\epsilon_{560 \text{ nm}}$
	$M^{-1} s^{-1}$		mM		$M^{-1} cm^{-1}$
Wild type ^c	1.13×10^5	0.46×10^5	2.2 ± 1.4	2750	1470
Y223S	1.5×10^5		6.5 ± 2.6	1050	400
Y223F	0.61×10^5		5.0 ± 2.2	3450	200

^a Determined in the presence of 20 mM sodium pyruvate and 400 mM ammonium chloride at pH 8.5, 25 °C.^b From the titration of the oxidized enzyme form with pyruvate, in 50 mM sodium pyrophosphate buffer, pH 8.5, 1% glycerol, and 400 mM ammonium chloride. The change in extinction is given for the $E_{ox} \cdot IA$ complex.^c Wild-type enzyme data are from Ref. 5, determined in 60 mM sodium pyrophosphate buffer, pH 8.5, containing 1.5% glycerol, 0.3 mM EDTA, and 0.75 mM 2-mercaptoethanol, at 25 °C.

tants bind the same ligands as wild type (Table II). There appears to be no clear trend to explain changes in K_d values for these ligands. These mutations result in no gross perturbations or loss of FAD. The changes we have measured in the kinetic properties of Y223F and Y223S are thus thought to be due to only specific and local structural modifications.

The rate at which Y223F is reduced by substrate ($k_2 = 1, 200 s^{-1}$) is about 3.5-fold faster than wild type. This result clearly eliminates Tyr-223 as a possible functional group playing a role in acid/base catalysis, *e.g.* in the abstraction of the α -carbon proton. No attempt will be made here to explain the increase in k_2 observed for the Y223F and Y223S mutants, although a similar effect was also reported for the Y143F mutant of flavocytochrome b_2 , a residue located at the interface between the flavodehydrogenase moiety and the heme-binding domain (27). Our data clearly show k_2 for these mutants to be at least as fast as the wild-type and that the hydroxyl group of Tyr-223 is not important for substrate oxidation. The slight decrease in k_{cat} for Y223F (60% of wild-type) appears to be a decrease in k_4 , the rate of product dissociation from oxidized enzyme (by using Equation 4, an approximate value of $k_4 = 254 s^{-1}$ can be calculated). Because $k_5 = 7.7 s^{-1}$ is very much slower than k_{cat} , k_5 clearly does not lie within the catalytic cycle, and the steady-state mechanism must be entirely ternary complex (inner loop of Scheme 1) and is described by Equations 1 and 2 (see above). Since k_2 is rate-limiting in catalysis for the wild-type enzyme, the overall reduction in k_4 is at least 10-fold the observed reduction in k_{cat} , or $k_4 \geq (350/210) (10) \geq 17$ -fold. For wild-type RgDAAO, D-alanine binding has been shown to be sticky ($k_2 > k_{-1}$) (5). Since binding never comes to equilibrium, the thermodynamic representation of substrate binding, K_d , is not nearly so important for substrate recognition as the rate of substrate association, k_1 . For a sticky substrate, the term $k_{red}/K_{d(\text{app})} = k_1 \cdot k_2 / (k_{-1} + k_2)$ (the slope of a double-reciprocal plot made from the data in Fig. 5 and not shown) reduces to k_1 . The value of $k_1 = 5.4 \times 10^4 M^{-1} s^{-1}$ estimated in this way for Y223F is only about one-half the value of wild-type enzyme, $1.2 \times 10^5 M^{-1} s^{-1}$ (5). All of the other kinetic constants we have measured for Y223F, including the reoxidation rate k_3 , are within a factor of 2–3 of the wild-type. Although there are some changes in binding, these are offset by the increased reduction rate of Y223F. Thus the catalytic efficiency, expressed as $k_{cat}/K_m(\text{D-Ala})$, of $9.8 \times 10^4 M^{-1} s^{-1}$ is quite similar to the wild-type enzyme, $1.3 \times 10^5 M^{-1} s^{-1}$ (5). The most significant change in the Y223F mutant is the >17-fold reduction in the rate of product dissociation from oxidized enzyme, k_4 . In general, the Y223F substitution results in only very minor changes in reactivity of the enzyme. The hydroxyl group of Tyr-223 is therefore not essential for catalytic activity, but it is important for substrate binding.

Substitution of serine at amino acid 223 produces more pronounced effects. The k_{cat} for Y223S is reduced 80-fold, and the reaction with D-alanine is essentially second-order with respect

to the substrate (although saturation kinetics are observed using D-valine as substrate). For a first-order mechanism, k_2 has been estimated at $\sim 1,400 s^{-1}$. This rate constant and the equation for a ternary complex mechanism (Equation 4) allow estimation of $k_4 = 4.2 s^{-1}$. The catalytic mechanism can be shown to still be a ternary complex for the Y223S mutant by comparison of the value of k_5 , product dissociation from reduced enzyme, with the value of flavin reduction and the equation of k_{cat} for the alternative ping-pong mechanism (see above). This is also supported by the finding of a converging line pattern in the Lineweaver-Burk plot (see Fig. 3). For k_4 to change from being not at all rate-limiting to being the slowest step in reduction, the overall change in k_4 must be at least 10-fold the change in k_{cat} . Thus k_4 is reduced at least (10) $(345 s^{-1}) / (4.2 s^{-1}) \geq 820$ -fold. Because k_4 represents the rate of product release from the reoxidized enzyme, it does not affect the steady-state Φ_{O_2} term (see Equations 1 and 2 and Table V).

Large perturbations in binding are also observed in the $K_{d(\text{app})}$ value from the reductive half-reaction of Y223S, which is ≈ 200 -fold greater with both D-alanine and D-valine than for wild-type RgDAAO. As discussed above for the Y223F mutant, $K_{d(\text{app})}$ approximates k_2/k_1 . The difference in k_2 is minor (only about 4.2-fold for D-alanine); therefore the majority of this change is due to the rate of substrate association, k_1 . This rate constant can be approximated by the value of $k_{red}/K_{d(\text{app})}$, which simplifies to k_1 when the substrate is sticky, and it is significantly slower than the corresponding value for the wild-type enzyme (Table IV). Although $K_{d(\text{app})}$ (and presumably the thermodynamic K_d) for D-alanine is substantially increased in Y223S, the K_m for the mutant is only twice that of wild type. This apparent discrepancy is easily resolved by substituting the known values into Equation 5 for $K_m(\text{D-Ala})$ (see Equations 1 and 2),

$$K_m(\text{D-Ala}) = k_4 \cdot (k_{-1} + k_2) / k_1 \cdot (k_2 + k_4) = k_4 \cdot K_{d(\text{app})} / (k_2 + k_4) \\ = (4.2 s^{-1} \cdot 0.71 M) / (1400 s^{-1} + 4.2 s^{-1}) = 2.1 \text{ mM} \quad (\text{Eq. 5})$$

The calculated value of 2.1 mM is one-third the measured K_m for D-alanine, a reasonable agreement considering the error in the estimation of k_2 . The rate of product release from the reduced enzyme, k_5 , is also changed in Y223S as follows: $35 s^{-1}$ for the mutant and $2.8 s^{-1}$ for wild-type enzyme. The IA product dissociates slower from oxidized, $4.2 s^{-1}$, than reduced enzyme, $35 s^{-1}$. As previously stated, this difference is not large enough to cause a change from a ternary complex to a ping-pong mechanism. Although the Y223S mutation causes no reduction in the chemical step in catalysis (k_2), substrate association (k_1) and product dissociation (k_4) are slowed. Clearly the phenol side chain is important for binding but not for the chemical step in catalysis. The changes in K_d for the binding of the competitive inhibitors reported in Table II (≈ 8 -fold weaker) correspond to $\approx 1.2 \text{ kcal mol}^{-1}$. This is possibly due to the lack of a single hydrogen bond between the hydroxyl group of Tyr-

223 and the carboxylate portion of the ligand.

Equation 2 defines the steady-state parameter $1/\Phi_{O_2} = k_2 k_3 / (k_2 + k_{-2})$. For an irreversible reaction such as that studied here, $k_{-2} = 0$, and $1/\Phi_{O_2}$ reduces to k_3 . For wild-type enzyme, $1/\Phi_{O_2}$ is equivalent to the independently measured value of k_3 , within experimental error (5). But for Y223S, k_3 is ~5-fold greater than $1/\Phi_{O_2}$, and for Y223F, k_3 is ~7-fold less than $1/\Phi_{O_2}$. In the case of a ping-pong mechanism, the appropriate rate equation defines $1/\Phi_{O_2} = k_6$. The low correspondence between $1/\Phi_{O_2}$ and measured k_3 values could be interpreted as due to a change to a ping-pong mechanism. As discussed above, converging line patterns on Lineweaver-Burk plots and measurements of k_5 from the reductive half-reactions indicate these mutants still follow ternary complex mechanisms. We consider measurements of k_3 in the oxidative half-reaction to be significantly more accurate than estimates from turnover data at low oxygen concentration. Measurement of k_3 indicated no significant changes in oxygen reactivity for the mutant E_{red} -IA complexes. The discrepancies between $1/\Phi_{O_2}$ and k_3 values probably arise from experimental error for $1/\Phi_{O_2}$, not a change in steady-state mechanism.

In a preliminary sequence comparison, Tyr-223 of RgDAAO was considered homologous to Tyr-228 of the mammalian enzyme (14). A re-analysis indicates that Tyr-223 is homologous to Tyr-224 of pig kidney DAAO, the residue located on the flexible loop that adapts its conformation depending on the size of the ligand side chain (28). Tyr-238 in RgDAAO is thought to correspond to Tyr-228 of the mammalian enzyme. The function of Tyr-223 in the active site of RgDAAO is different from that of the tyrosine residues (Tyr-224 and Tyr-228) of pig kidney DAAO. In fact, both mutants Y224F and Y228F of the mammalian DAAO show a large decrease in k_{red} (30- and 100-fold lower than in the wild-type) but did not affect significantly the $K_{d(app)}$ for D-alanine (11). These substitutions modify the interaction of the reduced enzyme with the product iminopyruvate, as indicated by the observation that Y228F totally abolished the formation of the absorbance at 560 nm during the reduction process, absorbance typical of the complex between the E_{red} form and IA. Two tyrosine residues are also present at the active site of other flavoproteins, e.g. flavocytochrome b_2 (29), glycolate oxidase (30), and lactate monooxygenase (31). These enzymes have been proposed to work by a carbanion mechanism, and in each enzyme they play different roles in fine-tuning substrate interactions and enzyme activity. Their roles were investigated by site-directed mutagenesis experiments but only by the replacement with a phenylalanine (a non-disruptive mutation). We changed also the spatial arrangement in the active site using a serine.

Results from experiments with Y223F and Y223S RgDAAO mutants demonstrate that Tyr-223 is important for enzyme-substrate and enzyme-product interactions and that the aromatic ring is also important for steric reasons. The differences in properties between the two mutants suggest that the side chain at position 223 contributes by fixing the substrate in the correct orientation for efficient catalysis mainly by its shape and less than by its hydrogen-bonding or electrostatic properties. Since Tyr-223 is not essential for catalysis (it is not the

base required by a carbanion mechanism), it should be possible to manipulate the substrate specificity of this biocatalyst by either site-directed mutagenesis or by a combinatorial approach using random mutagenesis. These results show great promise for future exploitation of *R. gracilis* DAAO as an industrial catalyst for the optical resolution of racemic mixtures and for the bioconversion of substrates as large as cephalosporin C.

Acknowledgments—We are indebted to Dr. Sandro Ghisla (Universität Konstanz, Germany) for the kind hospitality to use the stopped-flow spectrophotometer. We also thank Dr. Vincent Massey (University of Michigan) and Dr. Sandro Ghisla for the critical review and helpful comments on the manuscript.

REFERENCES

- Pilone, M. S., and Pollegioni, L. (1998) *Recent Res. Dev. Biotechnol. Bioeng.* **1**, 285–298
- Pollegioni, L., Blodig, W., and Ghisla, S. (1997) *J. Biol. Chem.* **272**, 4924–4934
- Curti, B., Ronchi, S., and Pilone Simonetta, M. (1992) in *Chemistry and Biochemistry of Flavoenzymes* (Muller, F., ed), pp. 69–94, CRC Press, Boca Raton, FL
- Pollegioni, L., Falbo, A., and Pilone, M. S. (1992) *Biochim. Biophys. Acta* **1120**, 11–16
- Pollegioni, L., Langkau, B., Fischer, W., Ghisla, S., and Pilone, M. S. (1993) *J. Biol. Chem.* **268**, 13850–13857
- Pilone, M. S., Butò, S., and Pollegioni, L. (1995) *Biotechnol. Lett.* **17**, 199–204
- Stegman, L. D., Zheng, H., Neal, E. R., Ben-Yoseph, O., Pollegioni, L., Pilone, M. S., and Ross, B. D. (1998) *Hum. Gene Ther.* **9**, 185–193
- Miura, R., and Miyake, Y. (1988) *Bioorg. Chem.* **16**, 97–110
- Walsh, C. T., Schonbrunn, A., and Abeles, R. (1971) *J. Biol. Chem.* **248**, 6855–6866
- Mattevi, A., Vanoni, M. A., and Curti, B. (1997) *Curr. Opin. Struct. Biol.* **7**, 804–810
- Pollegioni, L., Fukui, K., and Massey, V. (1994) *J. Biol. Chem.* **269**, 31666–31673
- Mattevi, A., Vanoni, M. A., Todone, F., Rizzi, M., Teplyakov A., Coda, A., Bolognesi, M., and Curti, B. (1996) *Proc. Natl. Acad. Sci. U. S. A.* **93**, 7496–7501
- Mizutani, H., Miyahara, I., Hirotsu, K., Nishina, Y., Shiga, K., Setoyama, C., and Miura R. (1996) *J. Biochem. (Tokyo)* **120**, 14–17
- Faotto, L., Pollegioni, L., Cecilian, F., Ronchi, S., and Pilone, M. S. (1995) *Biotechnol. Lett.* **17**, 193–198
- Sambrook, J., Fritsch, E. P., and Maniatis, T. (1989) *Molecular Cloning: A Laboratory Manual*, 2nd Ed., Cold Spring Harbor Laboratory Press, Cold Spring Harbor, NY
- Pollegioni, L., Molla, G., Campaner, S., Martegani, E., and Pilone, M. S. (1997) *J. Biotechnol.* **58**, 115–123
- Laemmli, U. K. (1970) *Nature* **227**, 680–685
- Molla, G., Vegezzi, C., Pilone, M. S., and Pollegioni, L. (1998) *Protein Expression Purif.* **14**, 289–294
- Minnaert, K. (1965) *Biochim. Biophys. Acta* **110**, 42–56
- Massey, V. (1991) in *Flavins and Flavoproteins* (Curti, B., Ronchi, S., and Zanetti, G., eds) pp.59–66, Walter de Gruyter & Co., Berlin
- Gibson, Q. H., Swoboda, B. E. P., and Massey, V. (1964) *J. Biol. Chem.* **259**, 3927–3934
- Dalziel, K. (1969) *Biochem. J.* **114**, 547–556
- Massey, V., and Hemmerich, P. (1978) *Biochemistry* **17**, 9–16
- Massey, V., and Gibson, Q. H. (1964) *Fed. Proc. U. S. A.* **23**, 18–29
- Porter, D. J. T., Voet, J. G., and Bright, H. J. (1977) *J. Biol. Chem.* **252**, 4464–4473
- Strickland, S., Palmer, G., and Massey, V. (1975) *J. Biol. Chem.* **250**, 4048–4052
- Rouviere-Fourmy, N., Capeillere-Blandin, C., and Lederer, F. (1994) *Biochemistry* **33**, 798–806
- Todone, F., Vanoni, M. A., Mozzarelli, A., Bolognesi, M., Coda, A., Curti, B., and Mattevi, A. (1997) *Biochemistry* **36**, 5853–5860
- Xia, Z.-X., Shamala, N., Bethge, P. H., Lim, L. W., Bellamy, H. D., Xuong, N. H., Lederer, F., and Mathews, F. S. (1987) *Proc. Natl. Acad. Sci. U. S. A.* **84**, 2629–2633
- Lindqvist, Y., and Brändén, C. I. (1989) *J. Biol. Chem.* **264**, 3624–3628
- Müh, U., Williams, C. H. Jr., and Massey, V. (1994) *J. Biol. Chem.* **269**, 7994–8000